Hydrodynamic study of a CO_2 desorption column using computational fluid dynamics.

Sumudu Karunarathne*, Kristoffer Eikeseth, Lars Erik Øi

University of South-Eastern Norway, N-3901 Porsgrunn, Norway

sumudu.karunarathne@usn.no

Abstract

Desorption of CO_2 from the rich amine solvent is one of the main operations in the amine-based CO_2 capture process. Proper vapour and liquid flow through the packing materials would enhance the heat transfer that is needed for stripping CO_2 from solvent. This is achieved by increasing the surface area of the flowing solvent by using the packing material. In this study, the created CFD (Computational Fluid dynamics) model in OpenFOAM^{TM} was able to simulate the factors influencing TCM (Technology Centre Mongstad) desorption performance, including liquid distribution, wettability and film thickness within the packing material. Three scenarios were considered including a base case for a better understanding of the hydrodynamics in the desorption column. Two of these are to compare the influence of mass flow rates, while one is used to investigating potential improvement. Simulation revealed that introducing a deflector plate and CO_2 bypass tube has a positive hydrodynamic effect in the desorption column.

1. Introduction

Carbon dioxide (CO_2) capture using amine solvents is a matured technology and has been used in the natural gas industry for decades. Various research has been performed to investigate the feasibility of employing the technology in post-combustion CO_2 capture. Technology Centre Mongstad (TCM) in Norway is a test facility that enables examining new solvents and to perform many other CO_2 capture related activities.

The process of post-combustion CO_2 capture undergoes cyclic absorption and desorption of CO_2 as illustrated in Fig. 1. The 30% wt monoethanolamine (MEA) is a benchmark solvent that has been tested many times to explore its capabilities for capturing CO_2 (Martinez, *et al*. 2017). The efficiency of absorption and desorption depends on the mass and heat transfer in the absorption and desorption columns. Thus, hydrodynamic of gas/vapour and liquid through packing material plays a vital role has a greater influence on mass and heat transfer between gas and liquid phases. Ideally, the solvent flows through the packing material and spreads out as an even, thin film across the entire packing material surface. However, several factors may negatively influence the flow, including:

- Velocities and distribution of liquid as it enters the packing bed.
- Angled channels in the packing material may force flow against the desorption tower walls, creating thick and fast flowing channels of solvent.
- CO_2 rising through the column in a turbulent manner may disturb the wetted surfaces.
- Liquid holdup may occur, creating localized flooding.

The aim of this work was to create a CFD (Computational Fluid Dynamic) model able to simulate factors influencing TCM desorption column performance, including liquid distribution, wettability and film thickness within the packing material. A scaled down version of the actual geometry of TCM desorption column was considered in the simulations.

2. Literature

Computational fluid dynamic studies on gas and liquid flow through packing have been reported in literature. This section cites some of the work done in this field regardless of whether it is absorption or desorption. Niegodajew and Asendrych, 2016 discussed a CFD simulation of small laboratory test rig which has a random packed bed. A 2-fluid Eulerian model has been employed to determine the flow behavior and validated using the reference data from rig. Pham *et al.*, 2015 described an approach taken to simulate an absorber considering the complex structured packing geometry to a homogeneous porous material. The study revealed that the porous media CFD model could reflect hydrodynamics and gas–liquid interactions of structured-packings. Gbadago *et al.*, 2020 performed a CFD simulation of a packed bed industrial absorber with interbed liquid distributors.

A porous media was used to represent the packing material in CFD simulations to avoid the high computational cost associated with simulating a real structured packing.

Yang *et al.*, 2018 presented a CFD based column study in which Mellapak 250 Y was selected as the packing material in geometry due to its thorough characterization. A similar analysis was performed by Isoz, 2017 by considering the real geometry of Mellapak 250.X and Mellapak 250.Y to study the gas flow through the structured packing. Raynal *et al.*, 2004 showed the possible ways CFD can be used for hydrodynamics calculations, liquid holdup and pressure drop within structured packings. Haroun *et al.*, 2012 extended the work by including a computational analysis of mass transfer in structured packings.

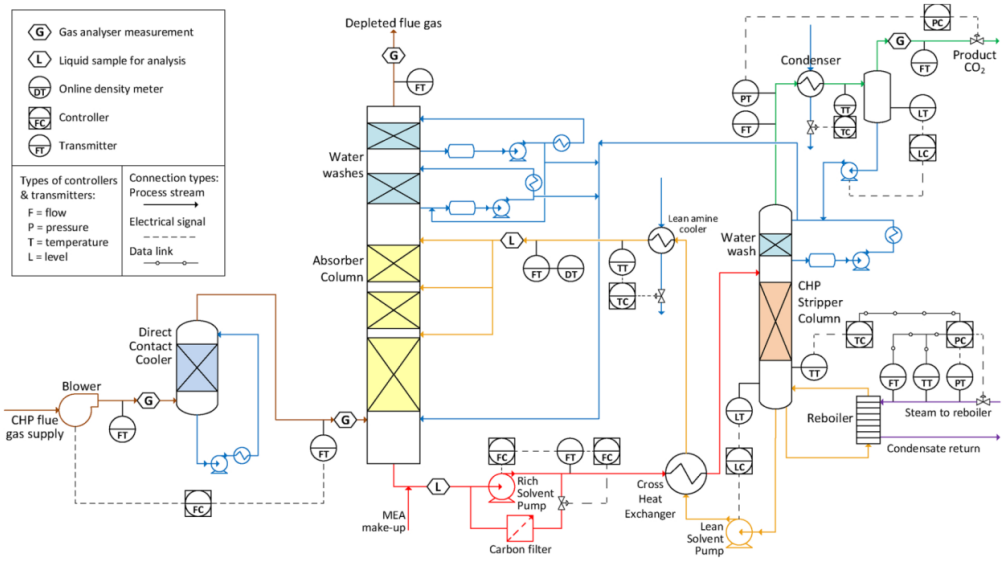

Figure 1: Process flow diagram of the TCM CO_2 capture facility. (Bui *et al.*, 2020)

3. Methodology

3.1. Geometry and Mesh

The geometry and mesh were created by using software tools Blender and SnappyHexMesh respectively. The simulation has been scaled down to make it viable to simulate with the available computing power. Symmetry is assumed to acquire a good representation of flow through the packing material and wall effects. The wall circumference to surface area ratio is not equal to the desorber design at TCM. This introduces some uncertainties in the study of hydrodynamic wall interface actions. The desorber at TCM has a packing bed height of 8 meters, has 28 packing bed layers and is 1.25 meters wide with 108 liquid distribution points. The performed simulation has been scaled down to a height of 0.92 meters with 3 packing bed layers and a width of 0.12 meters with 1 liquid distribution point. Fig. 2 illustrates a sectioned view of created geometry for simulations.

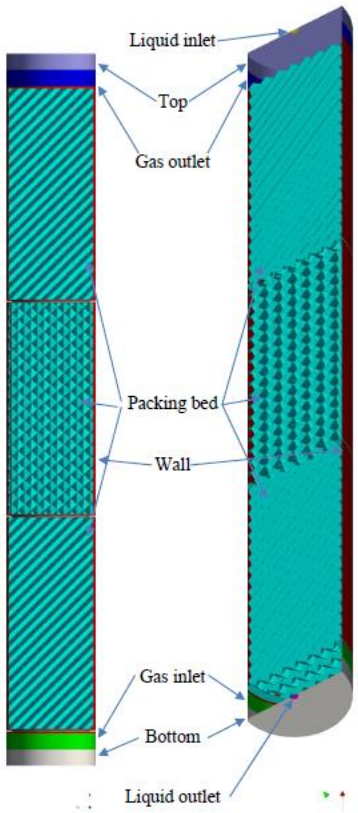

Figure 2: Sectioned view showing color-coded geometry, left = axis normal. Right = isometric view.

The mesh was created in two stages. First the geometry was created in Blender using a script created by Isoz, 2017 and modified to facilitate two-phase flow and geometries of the TCM desorption tower.
The SnappyHexMesh was used to create 3 sizes/types of cells as indicated below and matched them to the geometry as shown in Fig. 3,4 and 5.

- Layer 0 cells: cells further than 1.5 mm away from any surface, start as 1.5 mm hexahedral cells, but are formed and shaped to fit geometry as SnappyHexMesh runs.
- Layer 1 cells: cells closer than 1.5 mm to the surface, starting as 1.5 mm hexahedral cells, but are split into eight 0.75 mm hexahedral cells and formed and shaped to fit geometry as SnappyHexMesh runs.
- Surface layer cells: Added to surfaces of cylinder walls and packing material to achieve better results in simulations for gradients in velocity and film thickness. Two surface layers are added to the packing material, and one is added to the cylinder walls. Layer 1 and layer 0 cells are pushed back to accommodate surface layers as a surface layer addition, which is the last step of mesh generation in SnappyHexMesh.

The final mesh has 11.68 million cells in the layer 0 and 1 and 4.98 million cells in the surface layer with a total of 16.66 million cells. A mesh independence analysis has not been performed, but previous analysis on similar geometries has found 4 million cells per layer of packing material to be sufficient Isoz, 2017. These simulations have been performed with roughly 5.55 million cells per packing element.

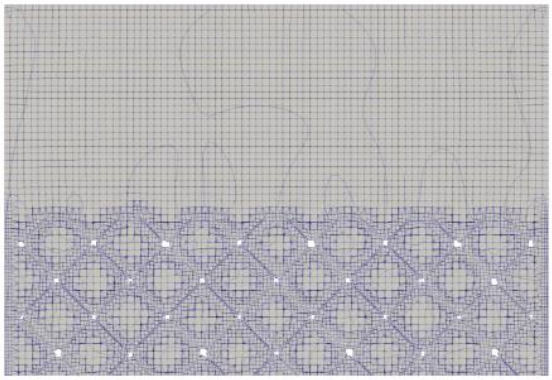

Figure 3: Sectioned view showing mesh at the top.

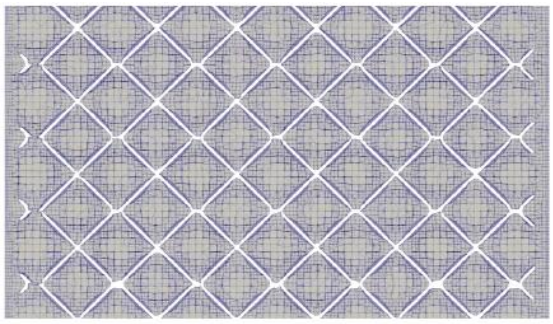

Figure 4: Sectioned view showing mesh in the middle.

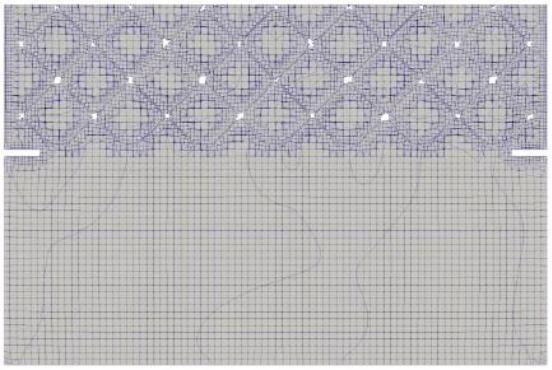

Figure 5: Sectioned view showing mesh at the bottom.

3.2. Mathematical models

The simulations were performed using the solver called InterFoam in OpenFOAM. It is a widely used solver for multiphase simulations of two incompressible, isothermal immiscible fluids in which VOF (volume of fluid) phase-fraction based interface capturing approach is adopted for computations (Heyns and Oxtoby, 2014).

Continuity Equation:

$$\frac{\partial u_j}{\partial x_j} = 0 \qquad 01$$

Where, u is velocity.

Momentum Equation:

$$\frac{\partial(\rho u_i)}{\partial t} + \frac{\partial(\rho u_j u_i)}{\partial x_j} = -\frac{\partial P}{\partial x_i} + \frac{\partial}{\partial x_j}\left(\tau_{ij} + \tau_{t_{ij}}\right) + \rho g_i + f_{\sigma i} \qquad 02$$

Where, g is gravitational acceleration, ρ is density, P is pressure, τ_{ij} is viscous stress, $\tau_{t_{ij}}$ is turbulent stress and $f_{\sigma i}$ is surface tension.

$$\rho = \alpha\rho_1 + (1-\alpha)\rho_2 \qquad 03$$

Here, α is 1 inside fluid 1 with the density ρ_1 and 0 inside fluid 2 with the density ρ_2. At the interphase between the two fluids α varies between 0 and 1.

The surface tension $f_{\sigma i}$ is modelled as continuum surface force (CSF) and calculated as follows.

$$f_{\sigma i} = \sigma\kappa\frac{\partial\alpha}{\partial x_i} \quad 04$$

σ is the surface tension constant and κ the curvature. The curvature can be approximated as follows:

$$\kappa = -\frac{\partial n_i}{\partial x_i} = -\frac{\partial}{\partial x_i}\left(\frac{\partial\alpha/\partial x_i}{|\partial\alpha/\partial x_i|}\right) \quad 05$$

Equation for the interphase:
An additional equation for α has to be solved in order to know where the interphase between the two fluids is,

$$\frac{\partial\alpha}{\partial t} + \frac{\partial(\alpha u_j)}{\partial x_j} = 0 \quad 06$$

The equation can be seen as the conservation of the mixture components along the path of a fluid parcel.

3.3 Simulations

Three simulation cases have been considered to investigate the desorber performance and archive a good understanding of the hydrodynamics. Tab. 1 lists the parameters considered in each simulation case while Tab. 2 provides thermophysical properties of CO_2 and MEA solvents.

Table 1: Specifications of the simulation cases.

Parameter	Base[a]	ICL07[a]	Defl_Exp
CO_2 mass flow rate (g/s)	7.70	8.07	4.00
MEA mass flow rate (g/s)	125.57	109.47	109.47
Geometry	TCM scale-down	TCM scale-down	TCM scale-down with added MEA Deflector plate

Reference (a): Bui *et al.*, 2020.

Both Base case and ICL07 have scaled-down values from plant operating parameters (Bui *et al.*, 2020). Base case is used as a reference for normal operating parameters, which is compared to ICL07, chosen because it gives a high CO_2 capture rate (Bui *et al.*, 2020).
The Delf_Exp is an experimental case where two potentially efficiency increasing factors were introduced:

i. A deflector plate is introduced into the stream of MEA before it enters the packing bed, the deflector plate may help in distributing MEA before it enters the packing bed, the MEA solvent may also become smaller droplets before entering the packing bed, thus releasing more CO_2 before entering the packing bed.
ii. The mass flow of CO_2 counterflowing MEA solvent through the packing bed is reduced to lower gas flow influence on liquid flow. In practice this might be accomplished by introducing a bypass pipe for CO_2 running parallel with the desorption tower along the top half of the packing bed.

Table 2: Thermophysical properties of CO_2 and MEA solvent.

Property	CO_2	Solvent
Temperature [K]	383	383
Density [kg/m^3]	1.384	1057[a]
Kinematic Viscosity [m^2/s]	1.37×10^{-5}	9.08×10^{-7}
Dynamic Viscosity [Pa·s]	1.83×10^{-5}	9.6×10^{-4} [b]
CO_2 loading (mol_{CO2}/mol_{MEA})		0.51[c]
MEA concentration (wt%)		27.5[c]

Reference (a): Han *et al.*, 2012; (b): Arachchige *et al.*, 2019; (c): Bui *et al.*, 2020.

The simulations were set to end at 7 seconds and results were taken at the 7th second as the final outcome in the simulation. All simulations were performed on virtualized Amazon AWS servers with 64 ARM cores of an AWS Gravitron3 CPU and 128 GB DDR5 RAM, giving a runtime of 72 hours per simulation.

3.4 Boundary conditions

Boundary conditions are necessary to solve governing equations. The solver used, InterFoam requires the following boundary conditions to be defined: Velocity (u), pressure (p), temperature (T) and turbulent volume fraction (α_{MEA}). The turbulence model, k-ε, requires the following boundary conditions to be defined: Turbulent kinetic energy (k), turbulent energy dissipation rate (ε) and turbulence viscosity (μ_t). Boundary conditions used are listed in Tab. 3 and 4.

4. Results

The pressure drop across the packed bed was examined in the different simulation cases. As shown in Fig. 6, the "base" case has the highest pressure drop of 605 Pa or 705 Pa/m. The simulation case "ICL07" has a pressure drop of 535 Pa or 624 Pa/m and "Defl_Exp" the lowest pressure drop of 366 Pa or 427 Pa/m.

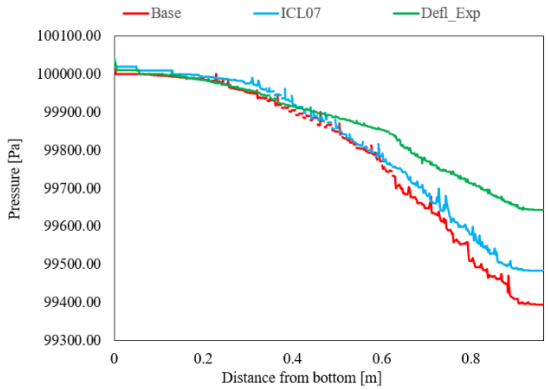

Figure 6: Comparison of pressure drop between cases.

It is remarked that even though "Delf_Exp" has half the gas flow of "ICL07", the pressure drop is not halved. Also, "Delf_Exp" has a smoother pressure graph, indicating low liquid hold-ups. This pressure drop is further illustrated in Fig.7 where the pressure is higher at the bottom and lower at the top of the column.

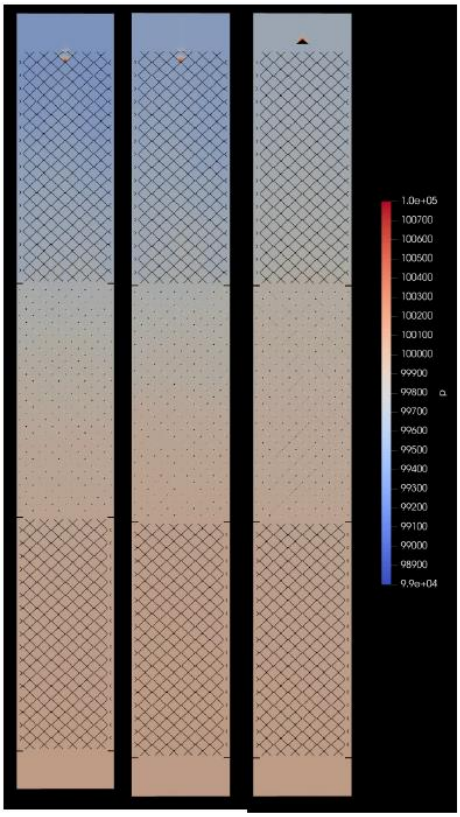

Figure 7: Sectioned view showing pressure, Left = "Base", Middle = "ICL07", Right = "Defl_Exp".

The simulated Base case and ICL07 case indicated severe liquid hold-up with large gatherings of liquid at certain points of the packing bed, while Defl_Exp case has some build-up, but it is not severe compared to other two cases as shown in Fig. 8. A smaller amount of liquid present in the bottom layer indicates the necessity of a longer runtime than 7 seconds to achieve an equilibrium condition in the simulation.

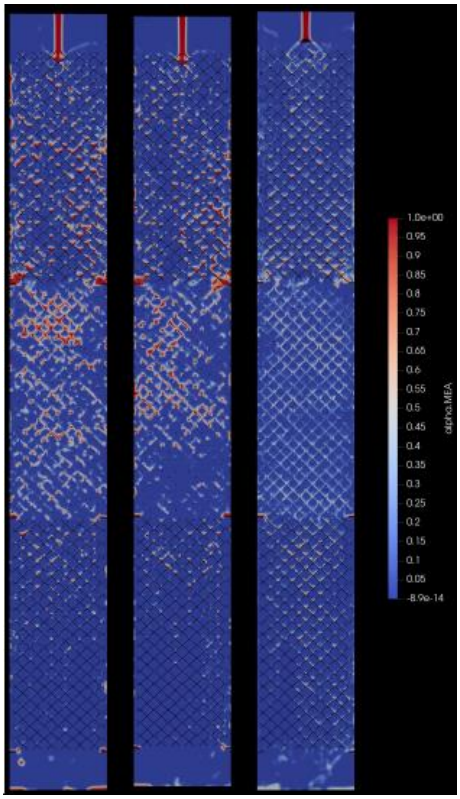

Figure 8: Sectioned view showing solvent distribution, Left = "Base", Middle = "ICL07", Right = "Defl_Exp".

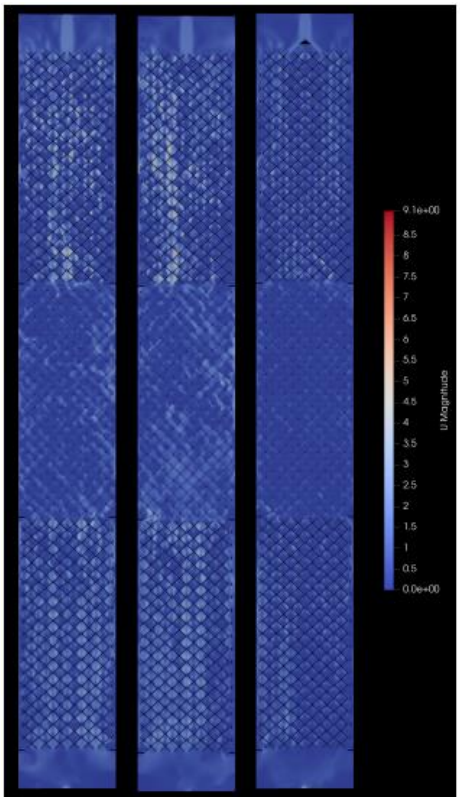

Figure 9: Sectioned view showing velocity, Left = "Base", Middle = "ICL07", Right = "Defl_Exp".

Fig. 9 illustrates the variation of gas velocity along the packed bed. A localized increase of velocity was observed in regions where less amount of liquid flows through the packing.

Table 3: Patch boundary conditions.

Variable	Liquid Inlet	Liquid Outlet	Gas Inlet	Gas outlet
u	flowRateInletVelocity constant	matchedFlowRateOutletVelocity Matched: Liquid Inlet	flowRateInletVelocity constant	matchedFlowRateOutletVelocity Matched: Gas Inlet
p_rgh	fixedFluxPressure	prghTotalPressure uniform 100000	fixedFluxPressure	fixedFluxPressure
T	fixedValue uniform 383	zeroGradient	zeroGradient	zeroGradient
k	fixedValue uniform 0.01	inletOutlet	fixedValue uniform 0.01	inletOutlet
ε	fixedValue uniform 0.02	inletOutlet	fixedValue uniform 0.02	inletOutlet
α_{MEA}	fixedValue uniform 1	zeroGradient	fixedValue uniform 1	zeroGradient
μ_t	calculated	calculated	calculated	calculated

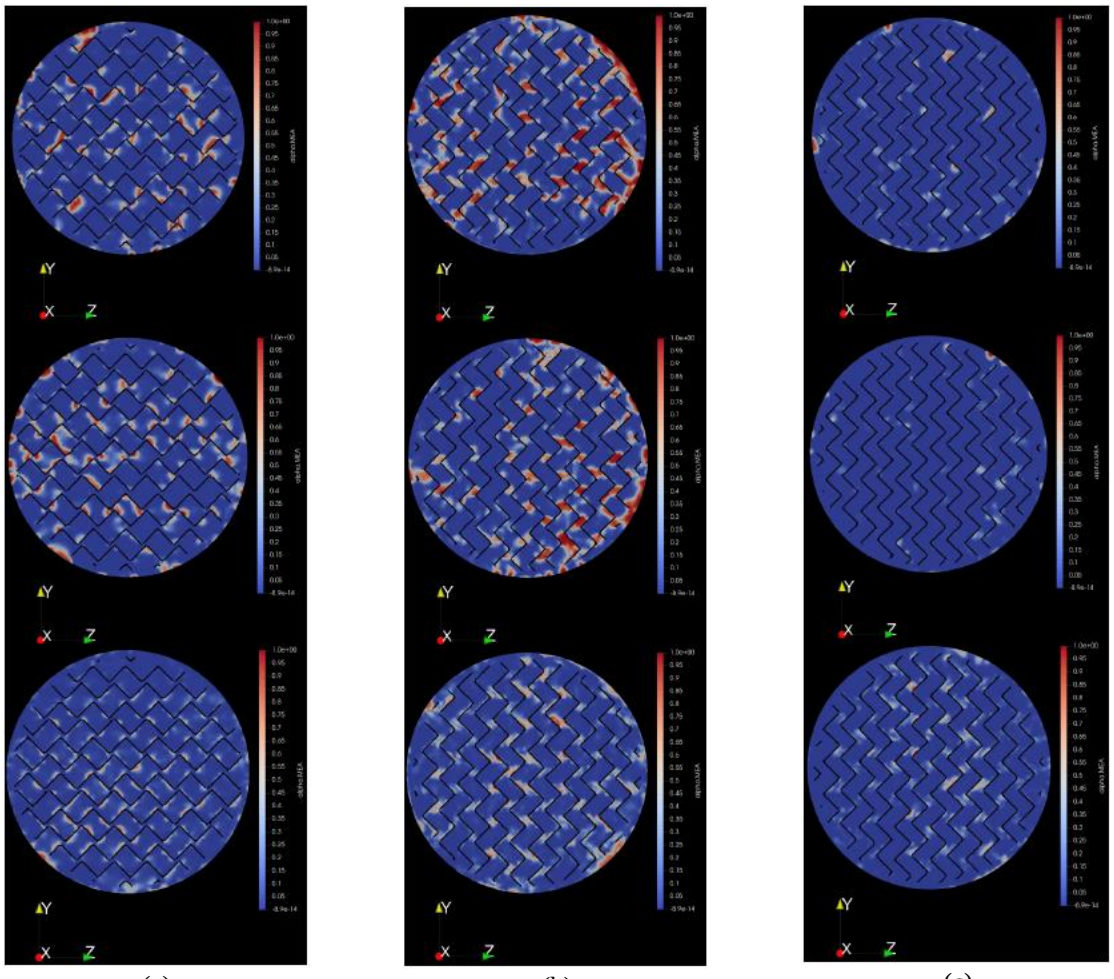

(a) (b) (c)

Figure 10: (a) Sectioned view showing MEA distribution at midpoint in the middle distribution bed layer, Top = “Base”, Middle = “ICL07”, Botom = “Defl_Exp”. (b) Sectioned view showing MEA distribution at midpoint in the top distribution bed layer, Top = “Base”, Middle = “ICL07”, Bottom = “Defl_Exp”. (c) Sectioned view showing MEA distribution at midpoint in the bottom distribution bed layer, Top = “Base”, Middle = “ICL07”, Botom = “Defl_Exp”.

Table 4: Wall boundary conditions

Variable	Top	Cylinder	Packing Element	Bottom
u	noSlip	noSlip	noSlip	noSlip
p	fixedFlux Pressure	fixedFluxPressure	fixedFluxPressure	fixedFluxPressure
T	zeroGradient	zeroGradient	zeroGradient	zeroGradient
k	kqRWall Function	kqRWallFunction	kqRWallFunction	kqRWallFunction
ε	epsilonWallFunction	epsilonWallFunction	epsilonWallFunction	epsilonWallFunction
α_{MEA}	zeroGradient	zeroGradient	zeroGradient	zeroGradient
μ_t	nutkWall Function	nutkWallFunction	nutkWallFunction	nutkWallFunction

Fig. 10 confirms the phenomenon described in Fig.8 that Base case and ICL07 case show severe liquid hold-up with large gatherings of liquid at certain points of the packed bed. Fig. 8 illustrates the liquid hold-up in Defl_Exp case, which shows building up liquid in some regions, but it is not severe compared to the other two cases.

5. Conclusion

This work simulated the top 3 layers out of a total of 28 layers of the TCM desorption column. The performed simulations showed liquid hold-up in the top 3 layers of the TCM desorption column packing bed when it was operated under normal operating parameters. Further it showed that introducing a deflector plate and/or a CO_2 bypass reduces simulated liquid hold-up, but the effect of deflector plate or CO_2 bypass had not been analyzed individually.

As the MEA flows down and releases CO_2 there is a decrease in both MEA and CO_2 mass flow, while also the distribution point(s) has less influence as the liquid flows through the 28 layers in the packing bed. It is therefore likely that the optimal operating conditions for one point in the desorption column yields suboptimal conditions above/below that point.

The simulated results were not verified using experimental data. Accordingly, such investigation is proposed as a future work by using publicly available plant operating data of TCM.

Acknowledgment

The authors gratefully acknowledge the staff of Technology Center Mongstad DA, Gassnova, Equinor, Shell and TotalEnergies for their interest in this work and particularly for access to data from the TCM DA facility.

References

Arachchige, U. *et al.* (2019) 'Dynamic Viscosity of Partially Carbonated Aqueous Monoethanolamine (MEA) from (20 to 150) °C', Applied Chemical Engineering. 2 (2). doi: 10.24294/ace.v1i2.660.

Bui, M. *et al.* (2020) 'Demonstrating flexible operation of the Technology Centre Mongstad (TCM) CO_2 capture plant', International Journal of Greenhouse Gas Control, 93, p. 102879. doi: 10.1016/j.ijggc.2019.102879.

Gbadago, D. Q. *et al.* (2020) 'CFD simulation of a packed bed industrial absorber with interbed liquid distributors', International Journal of Greenhouse Gas Control. 95, p. 102983. doi: 0.1016/j.ijggc.2020.102983.

Han, J. *et al.* (2012) 'Density of Water (1) + Monoethanolamine (2) + CO_2 (3) from (298.15 to 413.15) K and Surface Tension of Water (1) + Monoethanolamine (2) from (303.15 to 333.15) K', J. Chem. Eng. Data. 57(4), pp. 1095–1103. doi: 10.1021/je2010038.

Haroun, Y. *et al.* (2012) 'Mass transfer and liquid hold-up determination in structured packing by CFD', Chemical Engineering Science. 75, pp. 342–348. doi: 10.1016/j.ces.2012.03.011.

Heyns, J. A. and Oxtoby O.F. (2014) 'Modelling surface tension dominated multiphase flows using the VOF approach' 2014. [Online].Available:https://api.semanticscholar.org/CorpusID:16036879.

Isoz, M. 'CFD Study of Gas Flow Through Structured Separation Columns Packings Mellapak 250.X and Mellapak 250.Y', Topical Problems of Fluid Mechanics, 2017.

Martinez, M. *et al.* (2017) 'Solvent selection and design for CO_2 capture – how we might have been missing the point' Sustainable Energy and Fuels. 1(10), pp. 2078-2090. doi.org/10.1039/C7SE00404D.

Niegodajew, P. and Asendrych, D. (2016) 'Amine based CO_2 capture – CFD simulation of absorber performance', Applied Mathematical Modelling. 40(23), pp. 10222–10237. doi: 10.1016/j.apm.2016.07.003.

Pham, D. A. *et al.* (2015) 'Porous media Eulerian computational fluid dynamics (CFD) model of amine absorber with structured-packing for CO_2 removal', Chemical Engineering Science. 132, pp. 259–270. doi: 10.1016/j.ces.2015.04.009.

Raynal, L. *et al.* (2004) 'Liquid Holdup and Pressure Drop Determination in Structured Packing with CFD Simulations', The Canadian Journal of Chemical Engineering. 82, pp. 871-879.

Yang, L. *et al.* (2018) 'CFD Modeling on Hydrodynamic Characteristics of Multiphase Counter-Current Flow in a Structured Packed Bed for Post-Combustion CO2 Capture', Energies, 11, 3103. doi: 10.3390/en11113103.